© 2014. Published by The Company of Biologists Ltd | The Journal of Experimental Biology (2014) 217, 2201-2211 doi:10.1242/jeb.102129

RESEARCH ARTICLE

The four aldehyde oxidases of *Drosophila melanogaster* have different gene expression patterns and enzyme substrate specificities

Zvonimir Marelja[1], Miriam Dambowsky[1], Marco Bolis[2], Marina L. Georgiou[1], Enrico Garattini[2], Fanis Missirlis[3,*] and Silke Leimkühler[1,*]

ABSTRACT

In the genome of *Drosophila melanogaster*, four genes coding for aldehyde oxidases (*AOX1–4*) were identified on chromosome 3. Phylogenetic analysis showed that the AOX gene cluster evolved via independent duplication events in the vertebrate and invertebrate lineages. The functional role and the substrate specificity of the distinct *Drosophila* AOX enzymes is unknown. Two loss-of-function mutant alleles in this gene region, *low pyridoxal oxidase* (Po^{lpo}) and *aldehyde oxidase-1* ($Aldox\text{-}1^{n1}$) are associated with a phenotype characterized by undetectable AOX enzymatic activity. However, the genes involved and the corresponding mutations have not yet been identified. In this study we characterized the activities, substrate specificities and expression profiles of the four AOX enzymes in *D. melanogaster*. We show that the Po^{lpo}-associated phenotype is the consequence of a structural alteration of the *AOX1* gene. We identified an 11-bp deletion in the Po^{lpo} allele, resulting in a frame-shift event, which removes the molybdenum cofactor domain of the encoded enzyme. Furthermore, we show that AOX2 activity is detectable only during metamorphosis and characterize a *Minos-AOX2* insertion in this developmental gene that disrupts its activity. We demonstrate that the $Aldox\text{-}1^{n1}$ phenotype maps to the *AOX3* gene and AOX4 activity is not detectable in our assays.

KEY WORDS: Aldehyde oxidase, Molybdoenzymes, *Drosophila melanogaster*, Gene duplication, Substrate specificities

INTRODUCTION

Aldehyde oxidases (AOX; EC 1.2.3.1) belong to the family of molybdo-flavoenzymes together with the structurally related xanthine oxidoreductase (XOR) enzyme, which serves a key role in the catabolism of purines, metabolizing hypoxanthine into xanthine and xanthine into uric acid (Enroth et al., 2000). The structure of mouse AOX3 was shown to be highly identical to the homodimeric butterfly-shaped XOR enzymes, consisting of two identical 150 kDa subunits, with differences in the substrate binding pocket (Coelho et al., 2012). The structure of each monomer of these enzymes includes a 20 kDa N-terminal 2x[2Fe-2S] domain, a 40 kDa central FAD-containing domain and an 85 kDa C-terminal molybdenum cofactor (Moco) domain (Garattini et al., 2003; Mahro et al., 2011). The Moco of eukaryotic AOXs contains an equatorial sulfur ligand required for the catalytic activity of the enzymes (Wahl and Rajagopalan, 1982; Bray, 1988; Hille, 1996).

Most animal and plant genomes contain *AOX* gene clusters that arose from a series of duplication events from a common *XOR* ancestor (Forrest et al., 1956; Nash and Henderson, 1982; Rodríguez-Trelles et al., 2003; Garattini et al., 2008). Rodents and marsupials contain the largest number of *AOX* functional genes (*AOX1*, *AOX3*, *AOX4* and *AOX3L1*), whereas the human genome contains one single and functional *AOX1* gene (h*AOX1*) and two non-functional pseudogenes, representing the vestiges of the mouse *AOX3* and *AOX3L1* orthologs (Garattini et al., 2003; Garattini et al., 2008; Garattini et al., 2009; Kurosaki et al., 2013).

Mammalian AOXs are characterized by a broad substrate specificity, catalyzing the oxidation of various types of aldehydes and aza- and oxo-heterocycles of pharmacological and toxicological relevance (Schumann et al., 2009; Pryde et al., 2010; Garattini and Terao, 2011; Mahro et al., 2011; Garattini and Terao, 2012). The presence of some highly conserved residues in the catalytic centers and the high structural similarity between AOXs and XOR suggest common reaction mechanisms (Schumann et al., 2009; Coelho et al., 2012). Nevertheless, AOXs exhibit a broader substrate specificity than XOR (Pauff et al., 2009; Coelho et al., 2012). The physiological role and the endogenous substrates of human and mammalian AOXs are unknown.

In *Drosophila melanogaster*, the *rosy* (*ry*) locus encodes XOR (Chovnick et al., 1976; Keith et al., 1987). Loss-of-function *ry* mutants accumulate xanthine and hypoxanthine and are devoid of urate (Morita, 1958; Glassman and Mitchell, 1959), which makes them hypersensitive to oxidative stress (Hilliker et al., 1992). *Drosophila melanogaster ry* mutants are characterized by a dull reddish-brown eye colour because of the lowered concentrations of the red eye pigment drosopterin (bright red), and the increased chromogenic oxidation of the eye pigment dihydroxanthommatin (yellow brown) to xanthommatin (dull dark brown) (Phillips and Forrest, 1980). This suggests that the brownish eye color of the *ry* mutant arises from the progressive oxidation and degradation of eye pigments occurring in the absence of the antioxidant urate (Hilliker et al., 1992; Vorbach et al., 2003; Glantzounis et al., 2005). Metabolic profiling of the *Drosophila ry* and *maroon-like* (*ma-l*, suppressing Moco sulfuration and inactivating both XOR and AOXs) mutants confirmed the biochemical changes in xanthine, hypoxanthine and urate and revealed unsuspected changes in each of the tryptophan, arginine, pyrimidine and glycerophospholipid metabolic pathways (Kamleh et al., 2008; Kamleh et al., 2009).

Two loss-of-function mutant alleles, *low pyridoxal oxidase* (Po^{lpo}) and *aldehyde oxidase-1* ($Aldox\text{-}1^{n1}$), have been previously described to control AOX enzymatic activity (Collins and Glassman, 1969;

[1]Institute of Biochemistry and Biology, Department of Molecular Enzymology, University of Potsdam, 14476 Potsdam, Germany. [2]Laboratory of Molecular Biology, IRCCS-Istituto di Ricerche Farmacologiche Mario Negri IRCCS, via La Masa 19, 20157 Milan, Italy. [3]Departamento de Fisiología, Biofísica y Neurociencias, Centro de Investigación y de Estudios Avanzados, Av. IPN 2508, CP 07360 Mexico City, Mexico.

*Authors for correspondence (fanis@fisio.cinvestav.mx; sleim@uni-potsdam.de)

Received 7 January 2014; Accepted 20 March 2014

List of abbreviations

AOX	aldehyde oxidase
DHB	2,4-dihydroxybenzaldehyde
Moco	molybdenum cofactor
MTT	3-(4,5-dimethylthiazolyl-2)-2,5-diphenyltetrazoliumbromide
PLP	pyridoxal-5-phosphate
PO	pyridoxal oxidase
RNAi	RNA interference
TMB	2,4,5-trimethoxybenzaldehyde
XOR	xanthine oxidoreductase

Dickinson, 1970; Dickinson and Gaughan, 1981). On the basis of the data available, it was proposed that Po^{lpo} and $Aldox\text{-}1^{n1}$ map to two distinct and unidentified *AOX* genes belonging to the cluster of four *AOX* genes present on *Drosophila* chromosome 3 (Adams et al., 2000; Garattini et al., 2008). At present, the identities of the *AOX* genes corresponding to Po^{lpo} and $Aldox\text{-}1^{n1}$ are unknown. In addition, it remains to be established whether all of the four predicted *Drosophila AOX* genes are functionally active. Finally, the physiological significance of the *Drosophila AOX* genes needs to be ascertained. With respect to this, pyridoxal, the dephosphorylated form of the active vitamin B6 metabolite, seems to be a specific substrate of the *Po* encoding enzyme pyridoxal oxidase (PO). In insects, the levels of pyridoxal are considered to be of particular physiological relevance (Stanulović and Chaykin, 1971; Browder and Williamson, 1976; Cypher et al., 1982).

In this study we used a native in-gel activity assay to analyze extracts from a variety of *D. melanogaster* strains, where AOX activities had been disrupted by mutation or RNA interference (RNAi). We cloned the classical Po^{lpo} allele and showed that PO is the product of the *Drosophila AOX1* gene. We also report experiments suggesting that the AOX2 activity is only present during metamorphosis and that two further AOX activities are associated with the *AOX3* gene. We show that *AOX1*, *AOX2* and *AOX3* are conserved in most *Drosophila* species. Finally, we provide evidence that *AOX4* is evolutionarily more recent and that the activity of the encoded enzyme is undetectable in *D. melanogaster* extracts using a wide variety of substrates.

RESULTS

The *AOX* genes evolved by gene duplication events

Sequencing of the *D. melanogaster* genome led to the annotation of four genes, *CG18522*, *CG18519*, *CG6045* and *CG18516*, coding for an equivalent number of predicted proteins having all the structural characteristics of the AOX enzymes. In this study, we adopted the same nomenclature given to the four genes by Garattini et al. (Garattini et al., 2008): *AOX1* (CG18522), *AOX2* (CG18519), *AOX3* (CG6045) and *AOX4* (CG18516). Fig. 1 illustrates that these genes are clustered on chromosome 3R, 2.5 Mbp downstream from the *XOR/ry* locus (Bridges and Brehme, 1944; Keith et al., 1987; Chovnick et al., 1990). Using appropriate cytogenetic markers, the Po^{lpo} and $Aldox\text{-}1^{n1}$ alleles were mapped to the cytogenetic region 88F-89A, 0.08 cM apart from each other (Nelson and Szauter, 1992). This mapping is consistent with the location of the *AOX* gene cluster. Fig. 1 also shows the transposon insertions and genomic deletion mutants (deficiencies) that were used in this study and PCR primers used for molecular analysis.

To reconstruct the evolutionary history, we performed a phylogenetic analysis on the predicted structures of the *AOX* genes and corresponding protein products in *Drosophila* using the available genomic sequencing data covering a total of 12 distinct lineages. Our phylogenetic reconstruction suggests that *Drosophila* AOX1 originated from an ancient *XOR* duplication, distinct from the one giving rise to vertebrate *AOX*s (Fig. 2). It is likely that this duplication resulted in the appearance of *AOX1*, which, subsequently, duplicated into *AOX2*. A further duplication event involving *AOX2* gave rise to *AOX3*. *Drosophila willistoni* and *Drosophila mojavensis* are endowed with a single *XOR* and three active *AOX* genes that are predicted to be the orthologs of *D. melanogaster AOX1*, *AOX2* and *AOX3* (see also supplementary material Fig. S1). These species are representative of the most ancient complement of *AOX*s in *Drosophila*. The subsequent evolutionary history of *AOX*s in the Drosophilidae is characterized by four distinct *AOX3* duplications (Fig. 2). *Drosophila virilis* is endowed by a species-specific *AOX3-D* in addition to *XOR*, *AOX1*, *AOX2* and *AOX3* (Fig. 2, supplementary material Fig. S1). In *Drosophila grimshawi*, two distinct duplications giving rise to *AOX2-D* and *AOX3-D2* are evident (Fig. 2, supplementary material Fig. S1).

A major evolutionary event is represented by a third *AOX3* duplication, which led to the origin of *AOX4* and is conserved among downstream lineages. The duplication led to the extant complement of the predicted molybdo-flavoenzymes present in *Drosophila simulans*, *Drosophila sechellia*, *D. melanogaster*, *Drosophila yakuba* and *Drosophila erecta*, which consists of *XOR*, *AOX1*, *AOX2*, *AOX3* and *AOX4* genes (Fig. 2, supplementary material Fig. S1). In *Drosophila ananassae*, a further *AOX3* duplication gave rise to *AOX3-D3* (Fig. 2, supplementary material

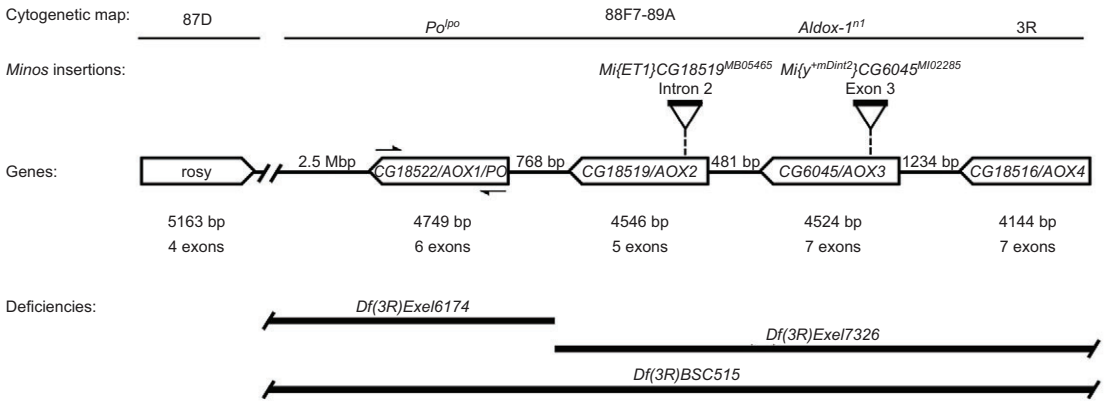

Fig. 1. Genomic location of the *Drosophila melanogaster AOX* genes. The genes *ry*/*XOR*, *CG18522*/*AOX1*, *CG18519*/*AOX2*, *CG6045*/*AOX3* and *CG18516*/*AOX4* are located on the right arm of the third chromosome (3R). Gene and inter-gene sizes are shown in bp and the number of exons per gene is indicated. The insertion points of *Mi{ET1}CG18519*^{MB05465} and *Mi{y*$^{+mDint2}$*}CG6045*^{MI02285} are shown and also the breakpoints for *Df(3R)Exel6174*, *Df(3R)Exel7326* and *Df(3R)BSC515*. The primers used to map the *lpo* mutation by sequencing are shown as arrows.

The Journal of Experimental Biology (2014) doi:10.1242/jeb.102129

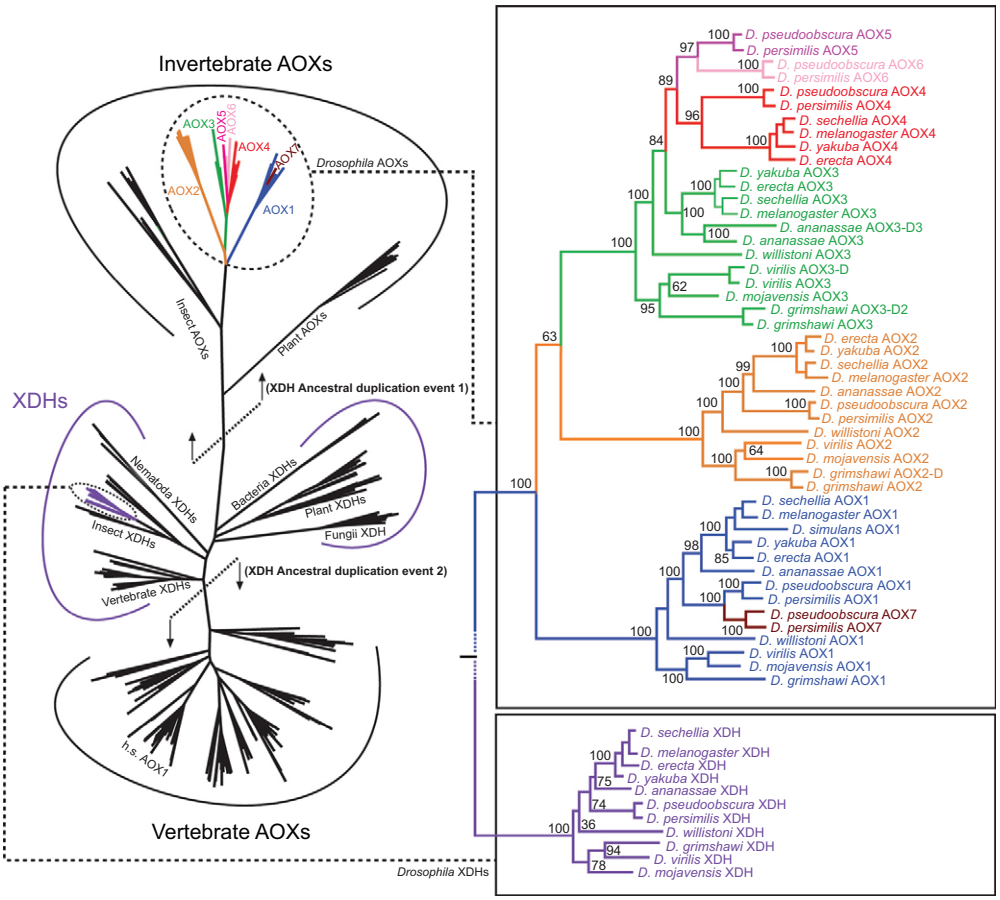

Fig. 2. Phylogenetic trees of the AOX and XOR proteins of Drosophilidae. The unrooted phylogenetic tree (left) was generated from combining *Drosophila* protein sequences with publicly available prokaryotic and eukaryotic AOX/XOR that are representative of different evolutionary lineages. The rooted phylogenetic tree (right) was generated from the reconstructed *Drosophila* AOX and XOR protein sequences. The unrooted phylogenetic tree consists of all the AOX and XOR proteins whose structure was deduced from genome sequencing data. The bootstrap scores for the most primitive branches of the rooted tree are shown. *Drosophila* XOR and the seven AOXs duplications are indicated with distinct colors.

Fig. S1). Finally, one deletion and three *AOX* duplications are predicted in the *Drosophila obscura* group, before the branching of *Drosophila pseudobscura* and *Drosophila persimilis*. In these lineages, *AOX3* is deleted while *AOX1* and *AOX4* are duplicated into *AOX7* and *AOX5*, respectively. In turn, *AOX5* is duplicated into *AOX6* (Fig. 2, supplementary material Fig. S1).

The use of different substrates reveals the presence of four aldehyde-catalyzing enzymes in adult wild-type flies

To evaluate whether the *AOX* genes predicted in *D. melanogaster* code for active proteins, we performed experiments on fly extracts. Proteins were separated by native PAGE and AOX activity was determined by an in-gel staining assay using various substrates and thiazolyl blue tetrazolium bromide (MTT) as the electron acceptor. With benzaldehyde as a substrate, four bands were detected (Fig. 3A). The top two bands constitute an incomplete resolved doublet (bands *a* and *b*). The enzyme-specific substrates pyridoxal, acetaldehyde and hypoxanthine indicate that the four bands are the products of the activity of distinct AOX isoenzymes. In addition, the results show that band *a* is stained exclusively in the presence of pyridoxal, while band *b* is stained only in the presence of acetaldehyde as a substrate (Fig. 3A). Band *c* is detectable only with acetaldehyde. Band *d* corresponds to XOR, as it is stained after incubation with hypoxanthine.

To relate each of the bands to the activity of the *AOX1–4* gene products, we evaluated the complement of bands in three fly strains lacking distinct genomic regions of the chromosome 3R affecting the *AOX* gene cluster (Fig. 1). *Df(3R)BSC515[AOX1-4]* removes all four *AOX* genes. Only *AOX1* is deleted in *Df(3R)Exel6174[AOX1]*, whereas in *Df(3R)Exel7326[AOX2-4]*, *AOX2–4* are deleted without affecting *AOX1*. We analyzed the trans-heterozygotes between the Deficiency (*Df*) chromosomes and the triple mutant recombinant ry^2, Po^{lpo}, *Aldox-1*^{n1} that removes all detectable AOX and XOR activity (Dickinson and Gaughan, 1981). Fly extracts of these genotypes were screened with 20 different substrates (Fig. 3B, supplementary material Fig. S2). Extracts of the homozygote *white* mutant were used as controls in our experiments, as they show the same four AOX/XOR bands observed in wild-type flies (see Fig. 3A). Out of the 20 substrates considered, salicylaldehyde, 2,4-dihydroxybenzaldehyde (DHB), 4-nitrobenzaldehyde and 2,4,5-trimethoxybenzaldehyde (TMB) are the most effective in distinguishing the various AOX bands. Similar to benzaldehyde (Fig. 3A), salicylaldehyde shows four bands (Fig. 3B). DHB highlights only the top three *a–c* bands, 4-nitrobenzaldeyhde only the two *b* and *c* bands, and TMB only the top *a* band (Fig. 3B). These results confirm that different *D. melanogaster* AOXs are characterized by different substrate specificities (Fig. 3B, supplementary material Fig. S2).

No bands stainable with the AOX substrates considered are detectable in *Df(3R)BSC515[AOX1-4]/ry*^{2}, Po^{lpo}, *Aldox-1*^{n1} mutant extracts. In contrast, the *Df(3R)Exel6174[AOX1]/ry*^{2}, Po^{lpo}, *Aldox-1*^{n1} mutant extracts only lack band *a*, suggesting that the *AOX1* gene codes for the classical PO enzyme. Instead of pyridoxal, TMB, previously shown to be specific for PO (Cypher et al., 1982), was used. In the *Df(3R)Exel7326[AOX2-4]/ry*^{2}, Po^{lpo}, *Aldox-1*^{n1} mutant extracts, bands *b* and *c* are not detectable. In the same mutant, the fastest migrating band *d* is visible when salicylaldehyde is used, contrary to what is observed in the *ry* mutant. This observation confirms previous studies that indicate that XOR can utilize certain AOX substrates (Dickinson and Gaughan, 1981). Finally, our results

The Journal of Experimental Biology (2014) doi:10.1242/jeb.102129

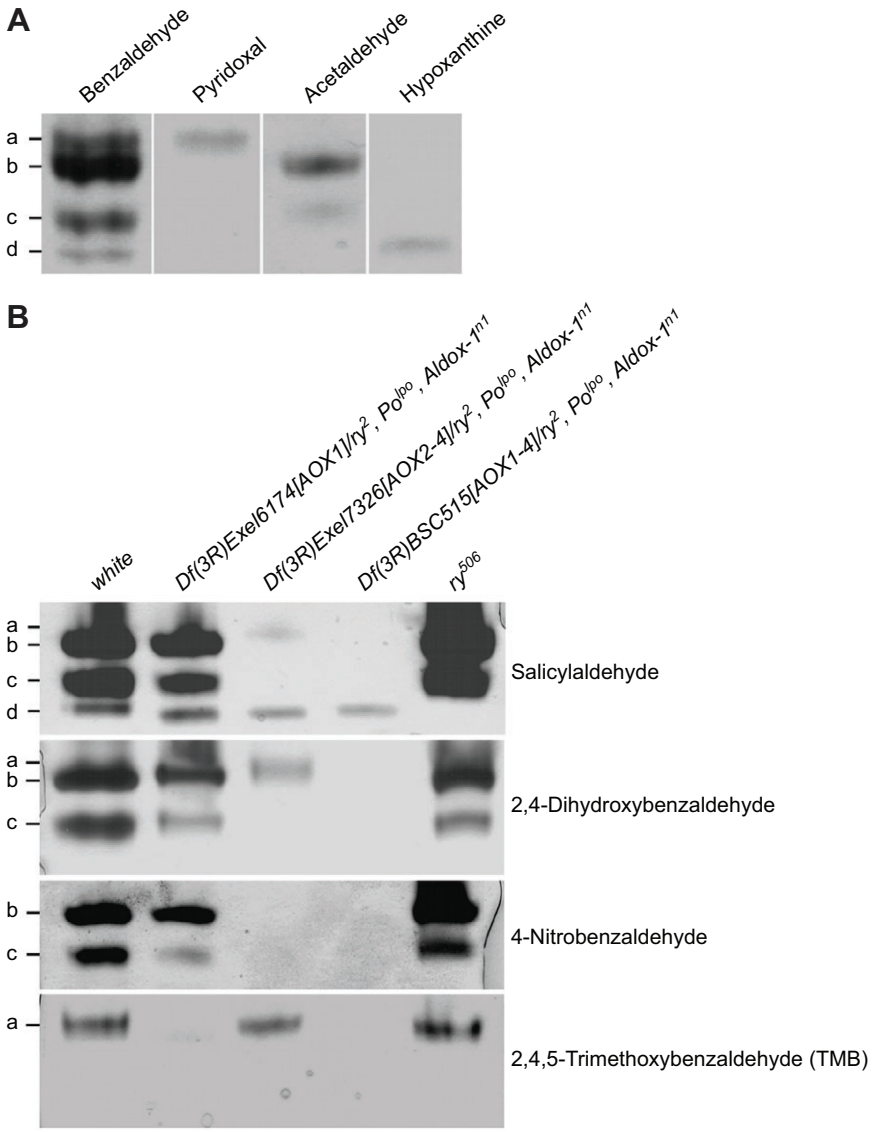

Fig. 3. Substrate specificities of the *D. melanogaster* AOXs. (A) The AOX and XOR activities in *white* fly extracts were analyzed in native gels in the presence of four different substrates with thiazolyl blue tetrazolium bromide and phenazine methosulfate as electron acceptors: with benzaldehyde the bands a–d were detected, with pyridoxal only band a was detected, with acetaldehyde bands b and c were detected, and with hypoxanthine band d was detected. (B) The same procedure was applied to the trans-heterozygotes *Df(3R)Exel6174[AOX1]/ry*^{2}, *Po*^{lpo}, *Aldox-1*^{n1}, *Df(3R)Exel7326[AOX2-4]/ry*^{2}, *Po*^{lpo}, *Aldox-1*^{n1} and *Df(3R)BSC515[AOX1-4]/ry*^{2}, *Po*^{lpo}, *Aldox-1*^{n1}. As controls, *white* and *rosy*^{506} (*ry*^{506}) mutant extracts were used. As substrates, salicylaldehyde, 2,4-dihydroxybenzaldehyde, 4-nitrobenzaldehyde and 2,4,5-trimethoxybenzaldehyde (TMB) were used.

show that bands *b* and *c* have the same substrate specificity, which might imply that these two bands are generated by the same protein (Fig. 3, supplementary material Fig. S2).

AOX1 is responsible for PO activity

To validate and extend the findings of the substrate screen, we further analyzed the AOX activity profiles in the deletion mutant *Df(3R)Exel6174[AOX1]/ry*^{2}, *Po*^{lpo}, *Aldox-1*^{n1} (Fig. 4A) and following ubiquitous *AOX1* silencing with a specific RNAi (Fig. 4B). Extracts from the control flies *Df(3R)Exel6174[AOX1]/TM6B,Tb*^{1}, *white* and *ry*^{506} show a specific AOX1 band following incubation with TMB. The band is absent in extracts of *Df(3R)Exel6174[AOX1]/ry*^{2}, *Po*^{lpo}, *Aldox-1*^{n1} flies (Fig. 4A). In contrast, the bands *b* and *c* observed with acetaldehyde as a substrate are present in the extracts of all control and mutant flies (Fig. 4A). Similarly, silencing of *AOX1* with a specific RNAi driven by the ubiquitous *act-Gal4* promoter in *white* flies annihilates the TMB-dependent band *a*, while it leaves unaffected the acetaldehyde-dependent bands *b* and *c* (Fig. 4B).

To further confirm that AOX1 is indeed the enzymatic activity missing in *Df(3R)Exel6174[AOX1]/ry*^{2}, *Po*^{lpo}, *Aldox-1*^{n1} flies, the wild-type *D. melanogaster AOX1* gene was cloned and the corresponding recombinant protein was expressed and purified in *Escherichia coli*. Recombinant AOX1 was used to compare the migration behavior and substrate specificity to that in the whole-fly extracts using in-gel staining analysis (Fig. 4C). As expected, recombinant AOX1 and whole-fly-extract band *a* co-migrate and are stained strongly with benzaldehyde/TMB and more weakly with acetaldehyde (Fig. 4C). Cloning and sequencing of the *AOX1* gene from *ry*^{2}, *Po*^{lpo}, *Aldox-1*^{n1} flies demonstrated an 11-bp deletion, which results in a frame-shift mutation that eliminates the Moco domain of *AOX1* (supplementary material Fig. S3). These results unequivocally demonstrate that the *AOX1* gene codes for the classical PO enzyme, which is inactivated in the *Po*^{lpo} mutant allele.

AOX3, the isoform affected by the *Aldox-1*^{n1} mutant allele, is likely to encode two protein variants

Acetylaldehyde-dependent bands *b* and *c* are absent in *Df(3R)Exel7326[AOX2-4]/ry*^{2}, *Po*^{lpo}, *Aldox-1*^{n1} mutant flies, confirming that the two bands must be the products of *AOX* genes other than *AOX1* (Fig. 5A). To identify the *AOX* gene responsible for the AOX activity associated with bands *b* and *c*, we used the *Minos* insertion mutant of the *AOX3* gene (*Mi-AOX3*; Fig. 1). Unlike extracts obtained for the *white*, *ry*^{506} and parental strains, the *Df(3R)Exel7326[AOX2-4]/Mi-AOX3* counterparts show no AOX

The Journal of Experimental Biology (2014) doi:10.1242/jeb.102129

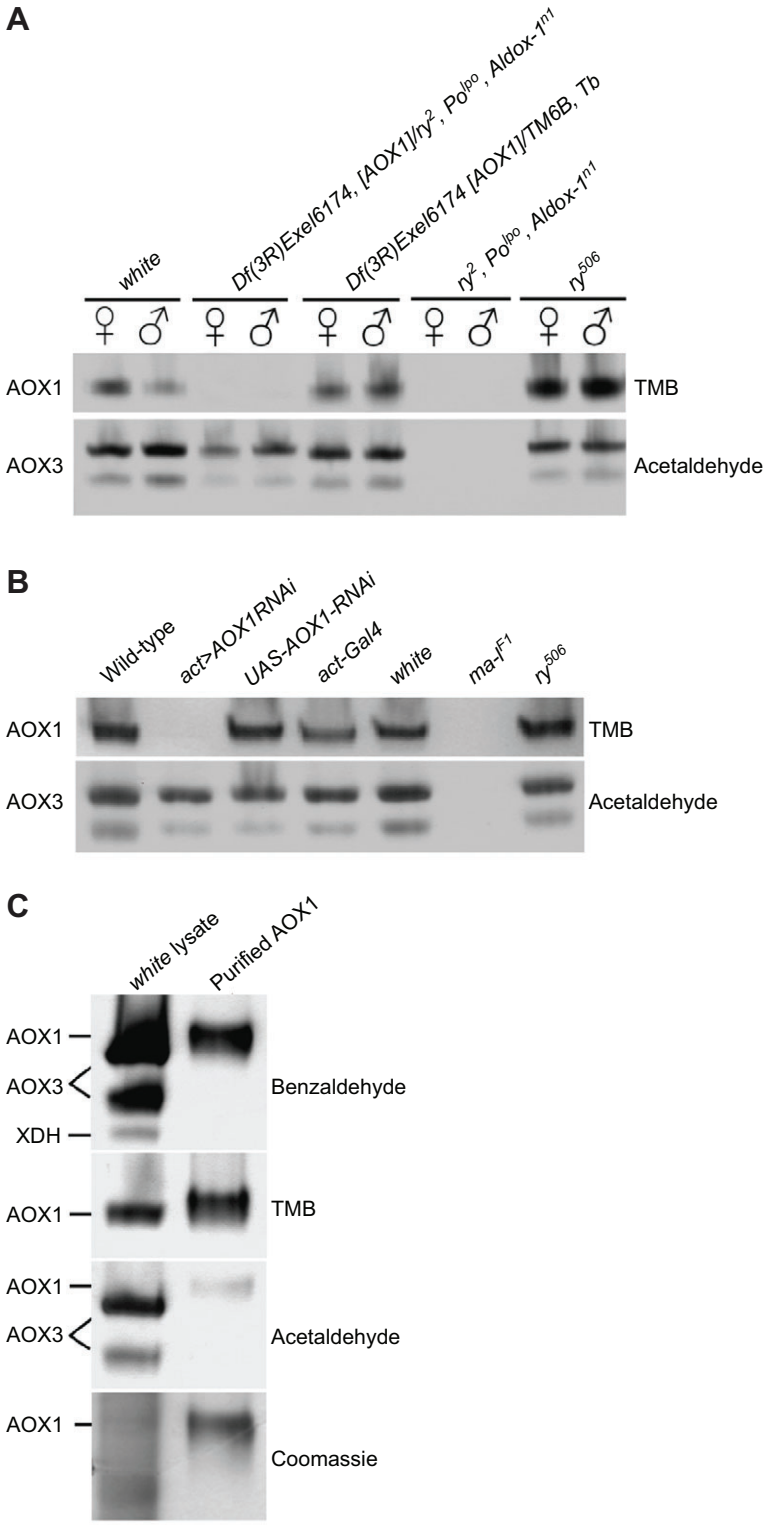

Fig. 4. Detection of the PO activity of the *AOX1* gene product. (A) Extracts from male and female *Df(3R)Exel6174[AOX1]/ry^{2}, Po^{lpo}, Aldox-1^{n1}* adult flies were analyzed for AOX1 and AOX3 activity. For AOX1 no activity was detectable with 2,4,5-trimethoxybenzaldehyde (TMB), whereas two bands were visualized with acetaldehyde, which correspond to the AOX3 activity (see also Fig. 5). The genotypes *white*, *ry^{506}* and the parentals *Df(3R)Exel6174[AOX1]/TM6B,Tb^{1}* and *ry^{2}, Po^{lpo}, Aldox-1^{n1}* were used as controls. (B) Ubiquitous silencing of AOX1 with act-Gal4 (*act>AOX1RNAi*) abolishes TMB-dependent activity, whereas the two bands that appear in the presence of acetaldehyde were not altered in comparison to the controls which were: *white*, *maroon-like^{F1}* (*ma-l^{F1}*), *ry^{506}* and the parentals *UAS-AOX1-RNAi* and *w^{1118}*; *act-Gal4*/*CyO* (*act-Gal4*). (C) Purified AOX1 (3 µg) was compared with endogenous activities from *white* fly extracts (40 µg total protein) using benzaldehyde, TMB and acetaldehyde as substrates. Coomassie stain was used to stain total proteins.

band upon incubation with acetaldehyde (Fig. 5B). Furthermore, silencing of the *AOX3* gene with a specific RNAi in adult *white* flies causes a strong reduction in the levels of the band *b* and the disappearance of band *c* (Fig. 5C). The intensity of the signal associated with the AOX1 band after incubation with TMB is comparable in *Df(3R)Exel7326[AOX2-4]/Mi-AOX3* and parental flies, demonstrating the specificity of the *AOX3* RNAi gene knock-down. The results are consistent with the idea that bands *b* and *c* are due to two separable protein products originating from the *AOX3* gene. At present, it is unclear whether the two forms of AOX3 are the products of alternative splicing events or the result of post-translational processing.

Tissue- and stage-specific expression of the catalytically active AOX iso-enzymes and corresponding mRNAs are generally correlated

The data produced by the modENCODE and FlyAtlas projects are accessible on FlyBase (http://flybase.org) and provide

The Journal of Experimental Biology (2014) doi:10.1242/jeb.102129

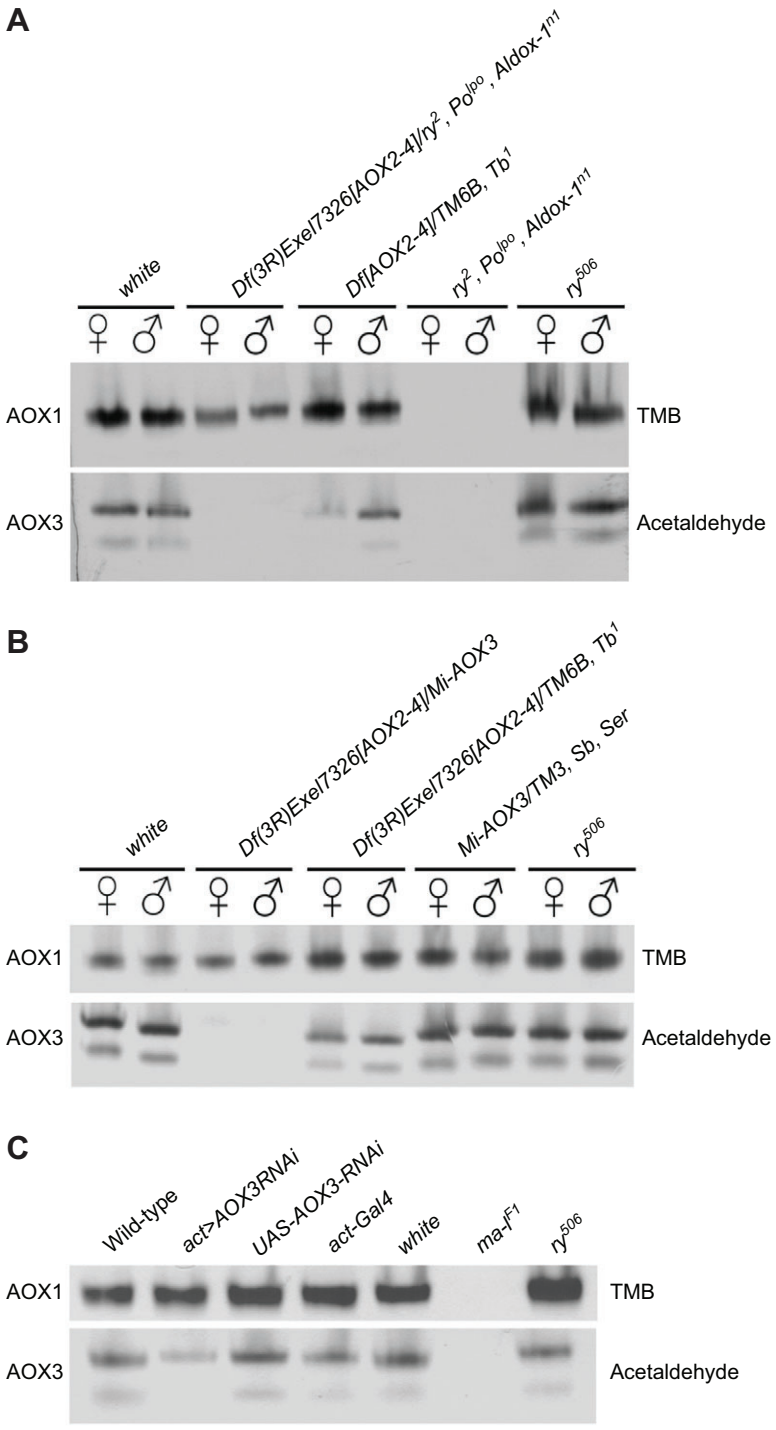

Fig. 5. Identification of the *AOX3*-dependent activities. Extracts from male and female *Df(3R)Exel7326[AOX2-4]/ry*^{2}*, Po*^{lpo}*, Aldox-1*^{n1} adult flies were analyzed for AOX1 and AOX3 activity. For AOX3, no activity was detectable with acetaldehyde, whereas the top band was visualized with TMB, which corresponds to the AOX1 activity (see also Fig. 4). The genotypes *white*, *ry*^{506} and the parentals *Df(3R)Exel7326[AOX2-4]/TM6B, Tb*^{1} and *ry*^{2}*, Po*^{lpo}*, Aldox-1*^{n1} were used as controls. (B) Extracts from male and female *Df(3R)Exel7326[AOX2-4]/Mi-AOX3* adult flies were analyzed for AOX1 and AOX3 activity. For AOX3, no activity was detectable with acetaldehyde, whereas the AOX1 band was visualized with TMB. As controls, the extracts of *white*, *ry*^{506} and the parentals *Df(3R)Exel7326[AOX2-4]/TM6B*, *Tb*^{1} and *Mi-AOX3/TM3, Sb, Ser* were used. (C) Ubiquitous silencing of AOX3 with act-Gal4 (*act>AOX3RNAi*) strongly reduces the acetaldehyde-dependent activity, whereas the AOX1 band that appears in the presence of TMB was not reduced. As controls, the extracts of *white*, *ma-l*^{F1}, *ry*^{506} and the parental *UAS-AOX3-RNAi* and *w*^{1118}; *act-Gal4*/*CyO* (*act-Gal4*) were used.

comprehensive information about the tissue- and stage-specific expression profiles of almost all the open reading frames identified in the *D. melanogaster* genome (Celniker et al., 2009; Robinson et al., 2013). Comparing the expression patterns of the various *AOX1*, *AOX2* and *AOX3* mRNAs (Fig. 6A), it is evident that *AOX1* is expressed throughout development, with peaks in the late embryonic stages, all the larval stages and during adulthood. *AOX3* mRNA is also measurable throughout development, with complementary peaks of expression relative to *AOX1*, i.e. during the early embryonic stages, in second and third instar larvae, in older pupae and in adult flies. *AOX2* shows low levels of expression in 10- to 16-h-old embryos and in third instar larvae, while large amounts of the transcript are expressed in 2-day-old pupae. *AOX4* is undetectable throughout development, while measurable levels of the transcript are present in adult head samples (FlyAtlas dataset).

To confirm some of the mRNA data at the protein level, we analyzed the profiles of AOX activity in extracts of different developmental stages (Fig. 6B). AOX1 was assayed with TMB, acetaldehyde was used for the detection of AOX3 and cinnamaldehyde was used as a common substrate to visualize all the AOX bands. Consistent with the mRNA data, high levels of AOX1 activity are detected in larvae and adult flies but low activities are seen in early embryos, white pre-pupae and pupae (2 to 3 days old).

The Journal of Experimental Biology (2014) doi:10.1242/jeb.102129

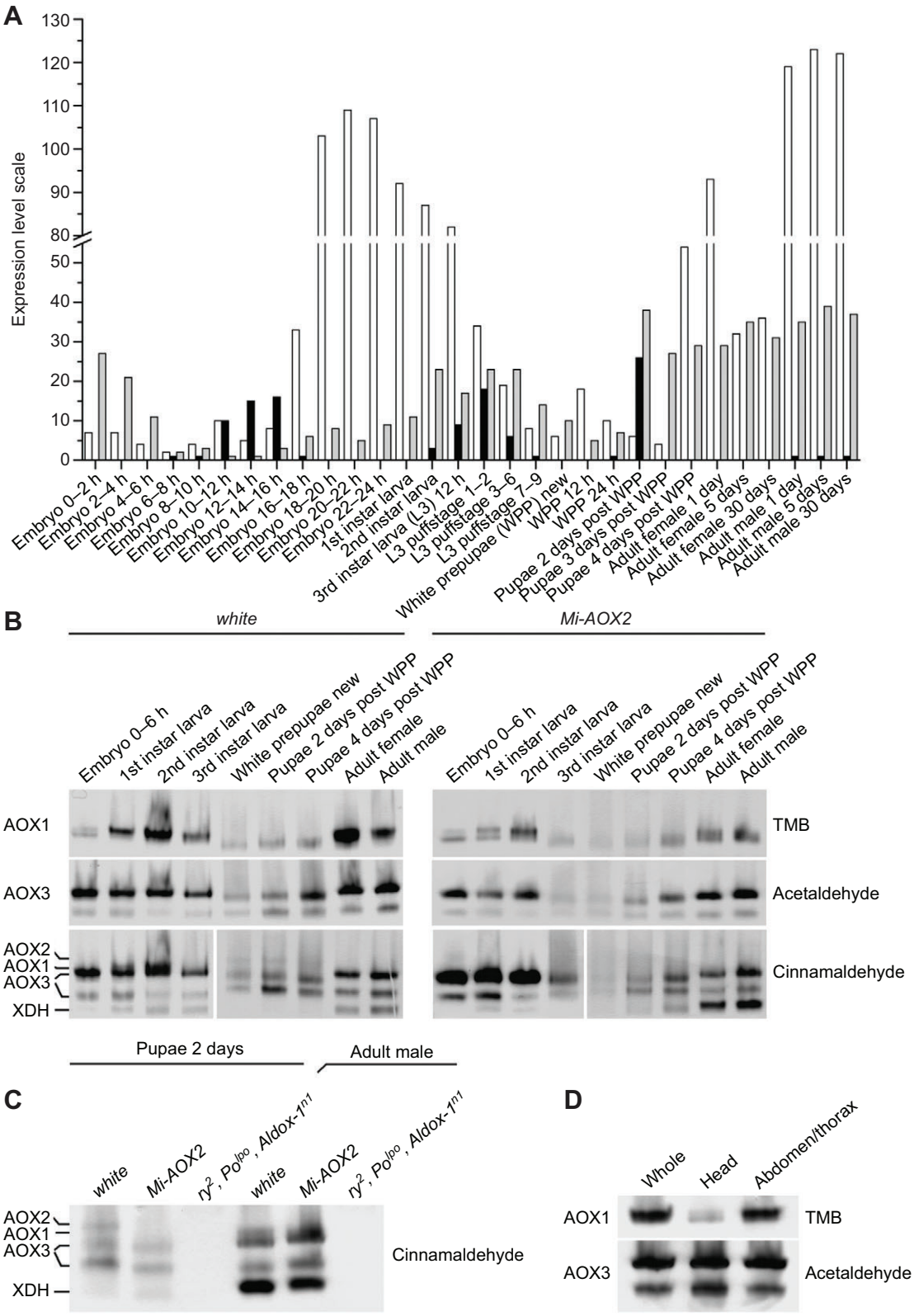

Fig. 6. Developmental expression pattern of *AOX1*, *AOX2* and *AOX3*. (A) The plot represents the modENCODE mRNA expression levels for *AOX1* (white bars), *AOX2* (black bars) and *AOX3* (gray bars) throughout the fly developmental stages (www.flybase.org). Expression level scale: 0–3, very low; 5–10, low; 10–25, moderate; 25–50, moderately high; 50–100, high; >100, very high. (B) Native activity gels were stained with TMB (for AOX1), acetaldehyde (for AOX3) and cinnamaldehyde (all AOXs and XOR). The enzyme activity patterns are shown at different developmental stages from the early embryo to the adult fly for *white* (left gel) and *Mi-AOX2* (right gel) strains. Note the appearance of the AOX2 activity in *white* pupae. (C) Comparison of AOX2 activity in extracts of 2-day-old pupae and in adult males of indicated genotypes. (D) AOX activities in extracts of decapitated flies (abdomen and thorax) and fly heads were analyzed with the substrates TMB and acetaldehyde.

The Journal of Experimental Biology (2014) doi:10.1242/jeb.102129

In contrast, AOX3 activity is high in early embryos, larvae, older pupae and adult flies, as expected from the *AOX3* mRNA profile.

Cinnamaldehyde reveals an additional band, which is observed in the pupae stages of the control *white* flies but not in the homozygous and viable *Minos-AOX2* insertion mutant (*Mi-AOX2*; Fig. 6B). This additional band is absent in the 2-day-old pupae of the ry^2, Po^{lpo}, $Aldox\text{-}1^{n1}$ mutant strains (Fig. 6C). The observation suggests that the $Aldox\text{-}1^{n1}$ locus impairs the expression of both the *AOX3* and *AOX2* genes.

We evaluated whether the expression of the *AOX4* mRNA in the head of the adult fly, as suggested by the FlyAtlas data, translates into the synthesis of catalytically active enzyme. To this purpose, we compared the AOX enzymatic profile in extracts obtained from the whole body, heads and thorax/abdomen of *white* flies. The results demonstrate no enrichment in AOX4 activity at the level of head samples (Fig. 6D). Interestingly, we observed that AOX1 activity is lower in the head and stronger in the abdomen/thorax. Taken together, these data indicate that there is a general correlation between the tissue- and stage-specific expression of the AOX mRNAs and corresponding catalytically active AOX iso-enzymes.

DISCUSSION

In previous studies, two genetic loci affecting *D. melanogaster* AOX activity were identified using the two loss-of-function mutant alleles Po^{lpo} and $Aldox\text{-}1^{n1}$, which are located in close proximity on the chromosomal region 88F-89A (Collins and Glassman, 1969; Dickinson, 1970; Dickinson and Gaughan, 1981; Nelson and Szauter, 1992). However, the available in-gel staining assays permitted the identification of only two AOX enzymes separable from XOR (Dickinson, 1970; Dickinson and Gaughan, 1981), (Warner et al., 1980; Warner and Finnerty, 1981). However, genome sequencing of *D. melanogaster* predicts a cluster of four *AOX* genes (*AOX1–4*) located ~2.5 Mbp downstream from the *rosy* locus on the right arm of the third chromosome (Fig. 1) (Adams et al., 2000; Garattini et al., 2008). This finding indicates that the initial characterization of AOX activities was incomplete and raises a number of questions regarding the physiological significance of all of these proteins in different tissues, their substrate specificities and their expression profiles during the development of the insect. In this study we reconstruct the phylogenesis of the *AOX* genes in *Drosophila* (Figs 2, 7). In addition, we demonstrate that the *AOX1* gene encodes for PO (Fig. 4), and that the AOX3 activity is disrupted in the classical $Aldox\text{-}1^{n1}$ mutant (Fig. 5). Finally, we establish that the *AOX2* gene is expressed during metamorphosis (Fig. 6), while no enzymatic activity could be associated with the *AOX4* gene. To reach these conclusions, we used a combination of genetic and biochemical tools, including an optimized in-gel activity staining method, new transposon-induced alleles, deficiency chromosomes and the RNAi methodology.

Previous phylogenetic studies have indicated that the evolution of the *AOX* genes is the result of a series of gene duplication, pseudogenization and gene deletion events (Garattini et al., 2008; Kurosaki et al., 2013). The reconstruction of the evolutionary history of this family of genes in *Drosophila* indicates that *AOX*s have originated from an ancient duplication of *XOR*. This duplication is distinct from the one giving rise to vertebrate *AOX*s, suggesting that the *Drosophila AOX* genes are not directly related to the vertebrate counterparts. In contrast to the human genome, which contains only one functional *AOX* gene (Berger et al., 1995; Garattini et al., 2003; Garattini et al., 2008), the Drosophilidae genomes include up to six active *AOX* genes. The minimal and probably the most ancient complement of *AOX* genes, consisting of the *AOX1*, *AOX2* and *AOX3* loci, is observed in *D. virilis*, *D. mojavensis* and *D. willistoni* (Fig. 7). With the exception of *D. obscura* species group, which lacks *AOX3*, but has acquired *AOX5*, *AOX6* and *AOX7*, all the species analyzed are characterized by the presence of the *AOX1*, *AOX2* and *AOX3* genes. Out of the four *D. melanogaster AOX* genes, *AOX1*, *AOX2* and *AOX3* are expressed in an active form during different developmental stages of the insect. In contrast, *AOX4* is not present in all *Drosophila* species (Fig. 7). Furthermore, in *D. melanogaster*, whose genome is predicted to contain an active *AOX4* gene, no catalytically active AOX4 enzyme was detected in any of the organ and developmental stages considered. Whether *AOX4* has a specialized function in *D. melanogaster* and why *AOX3* was duplicated into *AOX3-D* (*D. virilis* species group), *AOX4* (*D. melanogaster* species group, and *D. ananassae*), *AOX3-D2* (Hawaiian *Drosophila* species group) and *AOX3-D3* (*D. ananassae*) are questions that remain open.

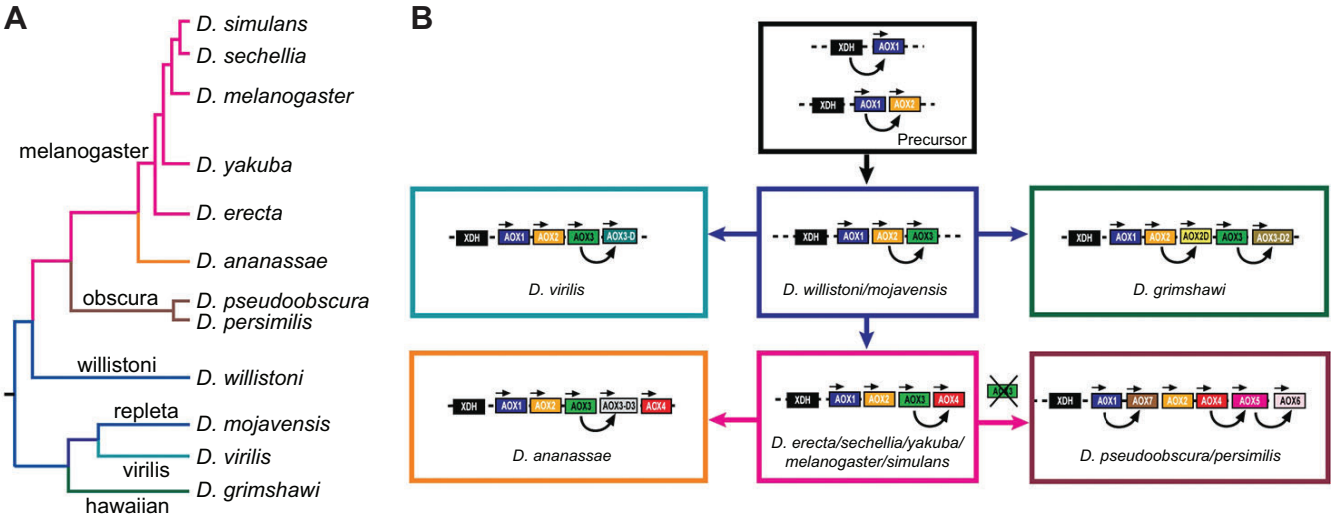

Fig. 7. Dynamic evolutionary history of the *Drosophila* AOX gene clusters. (A) The colored tree represents the inferred *Drosophila* phylogeny. (B) Schematic representation of the inferred evolutionary history of the AOX genes. Each panel indicates a different AOX complement and corresponding *Drosophila* species are indicated. The various AOX genes are represented in boxes; colors are associated with their corresponding tree branches shown in A. Predicted pseudogenes are crossed through. AOX orthologs are drawn in the same color. Curved black arrows indicate a duplication event.

The Journal of Experimental Biology (2014) doi:10.1242/jeb.102129

While we were able to show that the Po^{lpo} allele maps to the *AOX1* gene, the molecular nature of the *Aldox-1*^{n1} allele remains unknown. Further observations of the *ry*^{2}*, Po*^{lpo}*, Aldox-1*^{n1} mutant flies suggest that this mutant allele affects also *AOX2*, as 2-day-old *white* pupae are endowed with an additional AOX band, which is absent in the *ry*^{2}*, Po*^{lpo}*, Aldox-1*^{n1} and *Mi-AOX2* mutant flies (Fig. 6). Moreover, consistent with a former study on the *Aldox-1*^{n1} locus (Dickinson and Gaughan, 1981), we also detected a major and minor migrating band for AOX3 (indicated as band *b* and *c* in Fig. 3, supplementary material Fig. S2). Dickinson and Gaughan (Dickinson and Gaughan, 1981) suggested that two *Aldox*-dependent activities existed as modified minor band and unmodified major band forms. The cDNA sequences available in modENCODE support the presence of two alternative *AOX3* transcripts. One of them (NCBI accession AY094721) has a deletion of 226 amino acids from in the N terminus (Celniker et al., 2009). Therefore, we suggest that two AOX3 isoforms with distinct sizes are generated from the *AOX3* gene, which is consistent with the existence of two enzymatically active bands characterized by identical substrate specificities (Fig. 3, supplementary material Fig. S2). It is also possible that the faster band is a degradation product of AOX3. In this case, however, greater inter-sample variations in the intensity of the minor band to those observed would be expected.

The 20 substrates used in this study were selected among the molecules known to be oxidized by mammalian AOXs, although pyridoxal has been reported to be oxidized by fly extracts as well (Dickinson and Sullivan, 1975). The results obtained with these compounds indicate that *D. melanogaster* AOX1, AOX2 and AOX3 have different substrate specificities. It was previously shown that the homozygote *Aldox-1*^{n1} extracts (containing AOX1) have less than 2% of the wild-type AOX activity when acetaldehyde is used as substrate. In contrast, Po^{lpo} extracts (containing AOX3) present with levels of AOX activity that are close to those determined in wild-type flies (Dickinson and Gaughan, 1981; Cypher et al., 1982). We confirm these observations, demonstrating that acetaldehyde oxidation is detectable only in the presence of high amounts of purified recombinant AOX1 (Fig. 4C). In fly extracts acetaldehyde is specifically oxidized by AOX3. In contrast, AOX1 is the only enzyme capable of oxidizing pyridoxal or the benzaldehyde derivate TMB (Browder and Williamson, 1976; Cypher et al., 1982). We hypothesize that AOX1 plays a role in the decomposition of vitamin B6 from pyridoxal to 4-pyridoxic acid, which then might be excreted by the gut system (Forrest et al., 1961), as abundant amounts of the enzyme AOX1 are measurable in the midgut and Malphigian tubules (Dickinson and Gaughan, 1981) (FlyAtlas). Pyridoxal is one of the three natural forms of vitamine B6, along with pyridoxamine and pyridoxine. Pyridoxal is converted by the pyridoxal kinase into pyridoxal-5-phosphate (PLP), which acts as a cofactor for many enzymes involved in amino acid metabolism (Toney, 2005). Excess of vitamin B6 in the food might be countered by the action of AOX1, representing a competitive reaction to the pyridoxal kinase for the regulation of homeostatic levels of the PLP cofactor in the organism.

In the case of AOX1 and AOX3, we confirm the overlapping substrate specificities for a number of aldehydes, and aza- and oxo-heterocycles (Fig. 3, supplementary material Fig. S2) (Dickinson and Gaughan, 1981; Cypher et al., 1982). Interestingly, AOX2 activity is detectable with cinnamaldehyde but not with benzaldehyde (Fig. 6). These data support the idea that different AOX isoforms recognize a unique set of substrates and carry out different physiological tasks *in vivo*. In previous studies it was shown that the AOX enzymes in *Aldox-1*^{n1} and Po^{lpo} mutants have tissue-specific and overlapping expression patterns, which is also consistent with the modENCODE and FlyAtlas data presented in FlyBase (Dickinson and Gaughan, 1981; FlyAtlas). It was shown that the tissue distributions of AOX1 and AOX3 are overlapping and the two enzymes are synthesized predominantly in the midgut and Malpighian tubules. In contrast to AOX3, AOX1 is weakly expressed in the head (Fig. 6D) (Dickinson and Gaughan, 1981; FlyAtlas). In *D. melanogaster* whole-body extracts, a zymographic band corresponding to AOX4 cannot be identified, leading us to hypothesize that the *AOX4* gene exerts a tissue-specific function in the head of adult flies, as suggested by the mRNA expression data available in FlyAtlas (Robinson et al., 2013). However, our attempts to find a head-specific AOX4 have been inconclusive. Thus, we propose that AOX4 is either not expressed in an active form or its synthesis is restricted to sub-structures of the head, such as the antennae, precluding determination of the enzyme with our methodology. Reports demonstrating the presence of AOX enzymes in the antennae of several moth species are available (Rybczynski et al., 1989; Rybczynski et al., 1990; Merlin et al., 2005; Pelletier et al., 2007). In these studies, AOX activity has been detected in the antennae of both sexes, although larger amounts of the enzyme are present in male insects. Based on these observations, it has been proposed that antennae-specific AOXs may play a role in pheromone degradation. In this respect, it is interesting to note that the mammalian AOX3l1 enzyme may serve a similar function in rodents and dogs, as AOX3l1 is restricted to the olfactory mucosa and may function in the degradation of odorants and pheromones that are often aromatic aldehydes (Kurosaki et al., 2004; Terao et al., 2006; Kurosaki et al., 2013). It is remarkable that the AOX3l1 ortholog is a functionally inactive pseudogene in humans and primates, taxa whose olfactory system is less developed relative to rodents, dogs and insects.

In conclusion, we were able to distinguish the activities of AOX1, AOX2 and AOX3 in *D. melanogaster* and to confirm their complementary expression patterns during the different stages of the insect's development. We showed that the *AOX* gene cluster is under continuous evolutionary change in other species of *Drosophila*. However, the actual physiological functions of the *Drosophila* AOXs in different species, tissues and developmental stages remain unresolved.

MATERIALS AND METHODS

Chemicals

AOX substrates were obtained from Fluka, Sigma-Aldrich, Merck and Reachim: benzaldehyde, acetaldehyde, allopurinol, butyraldehyde, 2,4-dihydroxybenzaldehyde, 3-ethoxy-4-hydroxybenzaldehyde, heptaldehyde, 2-hydroxypyrimidine, hypoxanthine, *N*′-methylnicotinamide, 2,3-naphtalenedicarbaldehyde, 4-nitrobenzaldehyde, phenanthridine, phthalazin, pyridoxal-HCl, phenylacetaldehyde, salicylaldehyde, 2,4,5-trimethoxybenzaldehyde, valeraldehyde, vanillin, xanthine and trans-cinnamaldehyde.

Drosophila cultures

All flies used in this study were retrieved from public stock centers. Specifically, from the Vienna *Drosophila* RNAi Center (VDRC) (Dietzl et al., 2007), we used second chromosome insertion for *UAS-AOX1-RNAi* and an insertion on the X chromosome for *UAS-AOX3-RNAi* (Table 1). To induce the RNAi, a ubiquitous *w**, *Actin5C-Gal4/CyO* (*act-Gal4*) driver line was used as described previously (Missirlis et al., 2003) (Table 1). From Bloomington *Drosophila* Stock Center (BDSC), we used *Minos* insertions disrupting *AOX2* and *AOX3*, respectively (Metaxakis et al., 2005): the stocks were here referred to as *Mi-AOX2* and *Mi-AOX3* (Table 1, Fig. 1A). In addition, three deficiency chromosomes were obtained from BDSC that had the following characteristics: (1) *Df(3R)Exel6174[AOX1]* uncovers

The Journal of Experimental Biology (2014) doi:10.1242/jeb.102129

Table 1. *Drosophila melanogaster* lines used in this study

Stock name	Genotype	Source[a]	Stock ID number[b]
UAS-AOX1-RNAi	*P{KK105948}VIE-260B*)	VDRC	100330
UAS-AOX3-RNAi	*P{GD16750}^{v48191}*	VDRC	48191
act-Gal4	*w*, Actin5C-Gal4/CyO*	BDSC	4414
Mi-AOX2	*w^{1118}; Mi{ET1}CG18519^{MB05465}*	BDSC	25450
Mi-AOX3	*y,w*; Mi{$y^{+mDint2}$}CG6045^{MI02285}/TM3,Sb^1,Ser^1*	BDSC	33191
Df(3R)Exel6174[AOX1]	*w^{1118};Df(3R)Exel6174,P{w^{+mC}}Exel6174/TM6B,Tb^1*	BDSC	7653
Df(3R)Exel7326[AOX2-4]	*w^{1118};Df(3R)Exel7326/TM6B,Tb^1*	BDSC	7980
Df(3R)BSC515[AOX1-4]	*w^{1118};Df(3R)BSC515/TM6C,Sb^1,cu^1*	BDSC	25019
ry^{506}	*ry^{506}*	BDSC	225
ma-l^{F1}	*ma-l^{F1}*	BDSC	180
Po^{lpo} Aldox-1^{n1}	*ry^2 Po^{lpo} Aldox-1^{n1} Sb^{sbd-2}*	BDSC	5125

[a]Stocks were retrieved from public stock centers: Vienna *Drosophila* RNAi Center (VDRC) or Bloomington *Drosophila* Stock Center (BDSC).
[b]Identity (ID) numbers of the used stock from the corresponding public stock centers.

specifically *AOX1*, (2) *Df(3R)Exel7326[AOX2-4]* uncovers *AOX2-4* without affecting *AOX1*, and (3) (*Df(3R)BSC515[AOX1-4]* uncovers all four *AOX* genes (Table 1, Fig. 1A). The classic mutations *Po^{lpo}* (Collins and Glassman, 1969) and *Aldox-1^{n1}* (Dickinson, 1970) were used from the compound, homozygous viable chromosome *ry^2, Po^{lpo}, Aldox-1^{n1}, Sb^{sbd-2}* obtained from BDRC (Table 1). Wild-type TAN3 (Sadraie and Missirlis, 2011) and *white* (Gutiérrez et al., 2013) were used as controls.

Cloning and purification of *Drosophila* AOX1

The cDNA clone LD37006 containing the cDNA of *D. melanogaster AOX1* (*CG18522*) was obtained from the Berkeley *Drosophila* Genome Project (BDGP) Gold cDNA collection of the *Drosophila* Genomics Resource Center, and the forward primer CATATGGCTGGAAG-AATTACAATCAACG and the reverse primer GTCGACCTAAT-TGAGCTTGAACTGGCTG were used, which allowed cloning into the *Nde*I-*Sal*I sites of the expression vector pTrcHis (Temple et al., 2000). The resulting plasmid was designated pZM171 and expresses AOX1 with an N-terminal His_6-tag fusion. The plasmid pZM171 was transformed into *E. coli* TP1000 cells and His_6-AOX1 was heterologously expressed. The recombinant protein was purified by affinity chromatography using nickel-nitrilotriacetic acid (Ni-NTA) resin (QIAGEN, Valencia, CA, USA) and by a Superose 12 size exclusion chromatography column (GE Healthcare).

Production of fly extracts

For each sample, 10 flies, 10 abdomens, 50 heads, 200 embryos, 100 first instar larvae, 20 s instar larvae, 10 third instar larvae or 10 pupae were collected in a 1.5 ml Eppendorf tube, shock-frozen in liquid N_2 and stored at −80°C until further usage. For the preparation of fly extracts, a micro grinder (Sigma), composed of a battery-driven Pellet pestles cordless motor and Pellet pestles blue polypropylene sticks, was used. A volume of 8 µl per adult fly, larvae or pupae (except: 2 µl per embryo; 4 µl per first larvae; 3 µl per head; 5 µl per abdomen) of 0.1 mol l^{-1} Tris-HCl (pH 8.0) lysis buffer additionally containing 100 µmol l^{-1} EDTA, 1 mmol l^{-1} DTT and 2× protease inhibitor cocktail (Roche) was added to the flies and homogenization was performed for 30 s. The crude extract was centrifuged at 14,000 ***g*** for 10 min, the supernatant was transferred into a new 1.5 ml Eppendorf tube and a second centrifugation step was performed at 17,000 ***g*** for 10 min to remove additional cell debris. The homogenization procedure was carried out at 4°C.

Detection of in-gel AOX activity from fly extracts

To detect the activity of AOX enzymes in fly extracts, we performed a colorimetric in-gel activity assay. Here, 40 µg total protein of the whole fly extracts were separated by 6% native PAGE and the gels were subsequently stained for AOX activity using 5 mmol l^{-1} of a AOX substrate (see above), 0.4 mmol l^{-1} 3-(4,5-dimethylthiazolyl-2)-2,5-diphenyltetrazoliumbromide (MTT) and 0.1 mmol l^{-1} phenazine methosulfate (PMS). Upon AOX reaction, the reducing agent precipitates into a purple-black color, making it visible as band in the native gel.

Phylogenetic calculations

Using the *tBlastn* algorithm, we searched for exonic sequences coding for polypeptides with similarity to the *D. melanogaster* XOR, AOX1, AOX2, AOX3 and AOX4 proteins or an evolutionarily closer AOX, when necessary. Reconstruction of the *AOX* genes was performed, taking into account conservation of the coding exons in terms of sequence, length, and phase of exon/intron junctions. A major problem was sorting of genes coding for an active AOX protein (active genes) from pseudogenes, which may be transcribed, but do not encode a complete protein. *AOX* genes were considered as pseudogenes by the following criteria: (1) the presence of one STOP codon located in coding sequence; (2) the absence of one or more identifiable exons resulting in disruption of the expected downstream open reading frame; and (3) the lack of a recognizable intron/exon junction maintaining the open reading frame. To assign names to new previously unknown AOX isoenzymes, the following criteria were adopted: if duplications were detected in no more than one species, the '-D' suffix was added to the 'AOX' species that was likely to have originated it (i.e. *D. ananassae* AOX3 and *D. ananassae* AOX3-D); if the same AOX duplication event was detected in more than one lineage, a new name was given (i.e. AOX4 duplication in both *D. persimilis* and *D. pseudoobscura* was named AOX5).

To determine the evolution of the AOX genes, a phylogenetic analysis of the corresponding protein products was performed (12 taxa and 59 sequences, see supplementary material Table S1). Exonic structure, genomic loci and chromosomal position (if available) of the predicted genes were annotated. Multiple sequence alignments were prepared using Muscle (http://www.ebi.ac.uk/Tools/msa/muscle/) and visualized with CLC Main Workbench (http://www.clcbio.com/). The phylogenetic tree containing all the available *Drosophila* AOX and XOR protein structures was generated through the distance-based method BioNJ (http://www.atgc-montpellier.fr/bionj/) (Gascuel, 1997) and 100 bootstrap replicates were calculated. A comprehensive phylogenetic tree spanning from bacteria to vertebrates, generated through BioNJ, was based on publicly available prokaryotic as well as eukaryotic AOX and XOR protein sequences (see supplementary material Table S2) (Kurosaki et al., 2013).

Competing interests

The authors declare no competing financial interests.

Author contributions

Z.M., F.M. and S.L. designed the research. Z.M., M.D., M.L.G. and M.B. conducted the experiments and analyzed the data. Z.M., E.G., F.M. and S.L. wrote the paper.

Funding

This work was supported by the Deutsche Forschungsgemeinschaft (DFG) [grant number LE1171/8-1 to S.L.]; the Consejo Nacional de Ciencia y Tecnología project [grant number 179835 to F.M.]; by the European Molecular Biology Organisation (EMBO) [grant number ASTF 226-2011] and the Studienstiftung des deutschen Volkes (to Z.M.). A clone/plasmid for AOX1 cloning was obtained from the *Drosophila* Genomic Resource Center, supported by National Institutes of Health grant OD010949-10.

Supplementary material

Supplementary material available online at
http://jeb.biologists.org/lookup/suppl/doi:10.1242/jeb.102129/-/DC1

References

Adams, M. D., Celniker, S. E., Holt, R. A., Evans, C. A., Gocayne, J. D., Amanatides, P. G., Scherer, S. E., Li, P. W., Hoskins, R. A., Galle, R. F. et al. (2000). The genome sequence of *Drosophila melanogaster*. *Science* **287**, 2185-2195.

Berger, R., Mezey, E., Clancy, K. P., Harta, G., Wright, R. M., Repine, J. E., Brown, R. H., Brownstein, M. and Patterson, D. (1995). Analysis of aldehyde oxidase and xanthine dehydrogenase/oxidase as possible candidate genes for autosomal recessive familial amyotrophic lateral sclerosis. *Somat. Cell Mol. Genet.* **21**, 121-131.

Bray, R. C. (1988). The inorganic biochemistry of molybdoenzymes. *Q. Rev. Biophys.* **21**, 299-329.

Bridges, C. B. and Brehme, K. S. (1944). The mutants of *Drosophila melanogaster*. *Carnegie Institution of Washington* **552**, 252.

Browder, L. W. and Williamson, J. H. (1976). The effects of cinnamon on xanthine dehydrogenase, aldehyde oxidase, and pyridoxal oxidase activity during development in *Drosophila melanogaster*. *Dev. Biol.* **53**, 241-249.

Celniker, S. E., Dillon, L. A., Gerstein, M. B., Gunsalus, K. C., Henikoff, S., Karpen, G. H., Kellis, M., Lai, E. C., Lieb, J. D., MacAlpine, D. M. et al. (2009). Unlocking the secrets of the genome. *Nature* **459**, 927-930.

Chovnick, A., Gelbart, W., McCarron, M. and Osmond, B. (1976). Organization of the *rosy* locus in *Drosophila melanogaster*: evidence for a control element adjacent to the xanthine dehydrogenase structural element. *Genetics* **84**, 233-255.

Chovnick, A., Clark, S. H., Dutton, F. L., Jr and Reaume, A. G. (1990). The *rosy* locus and xanthine dehydrogenase in *Drosophila melanogaster*. *Prog. Clin. Biol. Res.* **344**, 1-18.

Coelho, C., Mahro, M., Trincão, J., Carvalho, A. T., Ramos, M. J., Terao, M., Garattini, E., Leimkühler, S. and Romão, M. J. (2012). The first mammalian aldehyde oxidase crystal structure: insights into substrate specificity. *J. Biol. Chem.* **287**, 40690-40702.

Collins, J. F. and Glassman, E. (1969). A third locus (ipo) affecting pyridoxal oxidase in *Drosophila melanogaster*. *Genetics* **61**, 833-839.

Cypher, J. J., Tedesco, J. L., Courtright, J. B. and Kumaran, A. K. (1982). Tissue-specific and substrate-specific detection of aldehyde and pyridoxal oxidase in larval and imaginal tissues of *Drosophila melanogaster*. *Biochem. Genet.* **20**, 315-332.

Dickinson, W. J. (1970). The genetics of aldehyde oxidase in *Drosophila melanogaster*. *Genetics* **66**, 487-496.

Dickinson, W. J. and Gaughan, S. (1981). Aldehyde oxidases of *Drosophila*: contributions of several enzymes to observed activity patterns. *Biochem. Genet.* **19**, 567-583.

Dickinson, W. J. and Sullivan, D. T. (1975). *Gene-Enzyme Systems in Drosophila*. Berlin: Springer-Verlag.

Dietzl, G., Chen, D., Schnorrer, F., Su, K. C., Barinova, Y., Fellner, M., Gasser, B., Kinsey, K., Oppel, S., Scheiblauer, S. et al. (2007). A genome-wide transgenic RNAi library for conditional gene inactivation in *Drosophila*. *Nature* **448**, 151-156.

Enroth, C., Eger, B. T., Okamoto, K., Nishino, T., Nishino, T. and Pai, E. F. (2000). Crystal structures of bovine milk xanthine dehydrogenase and xanthine oxidase: structure-based mechanism of conversion. *Proc. Natl. Acad. Sci. USA* **97**, 10723-10728.

Forrest, H. S., Glassman, E. and Mitchell, H. K. (1956). Conversion of 2-amino-4-hydroxypteridine to isoxanthopterin in *D. melanogaster*. *Science* **124**, 725-726.

Forrest, H. S., Hanly, E. W. and Lagowski, J. M. (1961). Biochemical differences between the mutants Rosy-2 and maroon-like of *Drosophila melanogaster*. *Genetics* **46**, 1455-1463.

Garattini, E. and Terao, M. (2011). Increasing recognition of the importance of aldehyde oxidase in drug development and discovery. *Drug Metab. Rev.* **43**, 374-386.

Garattini, E. and Terao, M. (2012). The role of aldehyde oxidase in drug metabolism. *Expert Opin. Drug Metab. Toxicol.* **8**, 487-503.

Garattini, E., Mendel, R., Romão, M. J., Wright, R. and Terao, M. (2003). Mammalian molybdo-flavoenzymes, an expanding family of proteins: structure, genetics, regulation, function and pathophysiology. *Biochem. J.* **372**, 15-32.

Garattini, E., Fratelli, M. and Terao, M. (2008). Mammalian aldehyde oxidases: genetics, evolution and biochemistry. *Cell. Mol. Life Sci.* **65**, 1019-1048.

Garattini, E., Fratelli, M. and Terao, M. (2009). The mammalian aldehyde oxidase gene family. *Hum. Genomics* **4**, 119-130.

Gascuel, O. (1997). BIONJ: an improved version of the NJ algorithm based on a simple model of sequence data. *Mol. Biol. Evol.* **14**, 685-695.

Glantzounis, G. K., Tsimoyiannis, E. C., Kappas, A. M. and Galaris, D. A. (2005). Uric acid and oxidative stress. *Curr. Pharm. Des.* **11**, 4145-4151.

Glassman, E. and Mitchell, H. K. (1959). Mutants of *Drosophila melanogaster* deficient in xanthine dehydrogenase. *Genetics* **44**, 153-162.

Gutiérrez, L., Zubow, K., Nield, J., Gambis, A., Mollereau, B., Lázaro, F. J. and Missirlis, F. (2013). Biophysical and genetic analysis of iron partitioning and ferritin function in *Drosophila melanogaster*. *Metallomics* **5**, 997-1005.

Hille, R. (1996). The mononuclear molybdenum enzymes. *Chem. Rev.* **96**, 2757-2816.

Hilliker, A. J., Duyf, B., Evans, D. and Phillips, J. P. (1992). Urate-null rosy mutants of *Drosophila melanogaster* are hypersensitive to oxygen stress. *Proc. Natl. Acad. Sci. USA* **89**, 4343-4347.

Kamleh, M. A., Hobani, Y., Dow, J. A. and Watson, D. G. (2008). Metabolomic profiling of *Drosophila* using liquid chromatography Fourier transform mass spectrometry. *FEBS Lett.* **582**, 2916-2922.

Kamleh, M. A., Hobani, Y., Dow, J. A., Zheng, L. and Watson, D. G. (2009). Towards a platform for the metabonomic profiling of different strains of *Drosophila melanogaster* using liquid chromatography-Fourier transform mass spectrometry. *FEBS J.* **276**, 6798-6809.

Keith, T. P., Riley, M. A., Kreitman, M., Lewontin, R. C., Curtis, D. and Chambers, G. (1987). Sequence of the structural gene for xanthine dehydrogenase (rosy locus) in *Drosophila melanogaster*. *Genetics* **116**, 67-73.

Kurosaki, M., Terao, M., Barzago, M. M., Bastone, A., Bernardinello, D., Salmona, M. and Garattini, E. (2004). The aldehyde oxidase gene cluster in mice and rats. Aldehyde oxidase homologue 3, a novel member of the molybdo-flavoenzyme family with selective expression in the olfactory mucosa. *J. Biol. Chem.* **279**, 50482-50498.

Kurosaki, M., Bolis, M., Fratelli, M., Barzago, M. M., Pattini, L., Perretta, G., Terao, M. and Garattini, E. (2013). Structure and evolution of vertebrate aldehyde oxidases: from gene duplication to gene suppression. *Cell. Mol. Life Sci.* **70**, 1807-1830.

Mahro, M., Coelho, C., Trincão, J., Rodrigues, D., Terao, M., Garattini, E., Saggu, M., Lendzian, F., Hildebrandt, P., Romão, M. J. et al. (2011). Characterization and crystallization of mouse aldehyde oxidase 3: from mouse liver to *Escherichia coli* heterologous protein expression. *Drug Metab. Dispos.* **39**, 1939-1945.

Merlin, C., François, M. C., Bozzolan, F., Pelletier, J., Jacquin-Joly, E. and Maïbèche-Coisne, M. (2005). A new aldehyde oxidase selectively expressed in chemosensory organs of insects. *Biochem. Biophys. Res. Commun.* **332**, 4-10.

Metaxakis, A., Oehler, S., Klinakis, A. and Savakis, C. (2005). Minos as a genetic and genomic tool in *Drosophila melanogaster*. *Genetics* **171**, 571-581.

Missirlis, F., Rahlfs, S., Dimopoulos, N., Bauer, H., Becker, K., Hilliker, A., Phillips, J. P. and Jäckle, H. (2003). A putative glutathione peroxidase of *Drosophila* encodes a thioredoxin peroxidase that provides resistance against oxidative stress but fails to complement a lack of catalase activity. *Biol. Chem.* **384**, 463-472.

Morita, T. (1958). Purine catabolism in *Drosophila melanogaster*. *Science* **128**, 1135.

Nash, D. and Henderson, J. F. (1982). The biochemistry and genetics of purine metabolism in *Drosophila melanogaster*. *Adv. Comp. Physiol. Biochem.* **8**, 1-51.

Nelson, C. R. and Szauter, P. (1992). Cytogenetic analysis of chromosome region 89A of *Drosophila melanogaster*: isolation of deficiencies and mapping of Po, Aldox-1 and transposon insertions. *Mol. Gen. Genet.* **235**, 11-21.

Pauff, J. M., Cao, H. and Hille, R. (2009). Substrate orientation and catalysis at the molybdenum site in xanthine oxidase: crystal structures in complex with xanthine and lumazine. *J. Biol. Chem.* **284**, 8760-8767.

Pelletier, J., Bozzolan, F., Solvar, M., François, M. C., Jacquin-Joly, E. and Maïbèche-Coisne, M. (2007). Identification of candidate aldehyde oxidases from the silkworm *Bombyx mori* potentially involved in antennal pheromone degradation. *Gene* **404**, 31-40.

Phillips, J. P. and Forrest, H. S. (1980) Ommochromes and pteridines. In *The Genetics and Biology of Drosophila,* Vol. 2 (ed. M. Ashburner and T. R. F. Wright), pp. 542-623. New York, NY: Academic Press.

Pryde, D. C., Dalvie, D., Hu, Q., Jones, P., Obach, R. S. and Tran, T. D. (2010). Aldehyde oxidase: an enzyme of emerging importance in drug discovery. *J. Med. Chem.* **53**, 8441-8460.

Robinson, S. W., Herzyk, P., Dow, J. A. and Leader, D. P. (2013). FlyAtlas: database of gene expression in the tissues of *Drosophila melanogaster*. *Nucleic Acids Res.* **41**, D744-D750.

Rodríguez-Trelles, F., Tarrío, R. and Ayala, F. J. (2003). Convergent neofunctionalization by positive Darwinian selection after ancient recurrent duplications of the xanthine dehydrogenase gene. *Proc. Natl. Acad. Sci. USA* **100**, 13413-13417.

Rybczynski, R., Reagan, J. and Lerner, M. R. (1989). A pheromone-degrading aldehyde oxidase in the antennae of the moth *Manduca sexta*. *J. Neurosci.* **9**, 1341-1353.

Rybczynski, R., Vogt, R. G. and Lerner, M. R. (1990). Antennal-specific pheromone-degrading aldehyde oxidases from the moths *Antheraea polyphemus* and *Bombyx mori*. *J. Biol. Chem.* **265**, 19712-19715.

Sadraie, M. and Missirlis, F. (2011). Evidence for evolutionary constraints in *Drosophila* metal biology. *Biometals* **24**, 679-686.

Schumann, S., Terao, M., Garattini, E., Saggu, M., Lendzian, F., Hildebrandt, P. and Leimkühler, S. (2009). Site directed mutagenesis of amino acid residues at the active site of mouse aldehyde oxidase AOX1. *PLoS ONE* **4**, e5348.

Stanulović, M. and Chaykin, S. (1971). Aldehyde oxidase: catalysis of the oxidation of N^1-methylnicotinamide and pyridoxal. *Arch. Biochem. Biophys.* **145**, 27-34.

Temple, C. A., Graf, T. N. and Rajagopalan, K. V. (2000). Optimization of expression of human sulfite oxidase and its molybdenum domain. *Arch. Biochem. Biophys.* **383**, 281-287.

Terao, M., Kurosaki, M., Barzago, M. M., Varasano, E., Boldetti, A., Bastone, A., Fratelli, M. and Garattini, E. (2006). Avian and canine aldehyde oxidases. Novel insights into the biology and evolution of molybdo-flavoenzymes. *J. Biol. Chem.* **281**, 19748-19761.

Toney, M. D. (2005). Reaction specificity in pyridoxal phosphate enzymes. *Arch. Biochem. Biophys.* **433**, 279-287.

Vorbach, C., Harrison, R. and Capecchi, M. R. (2003). Xanthine oxidoreductase is central to the evolution and function of the innate immune system. *Trends Immunol.* **24**, 512-517.

Wahl, R. C. and Rajagopalan, K. V. (1982). Evidence for the inorganic nature of the cyanolyzable sulfur of molybdenum hydroxylases. *J. Biol. Chem.* **257**, 1354-1359.

Warner, C. K. and Finnerty, V. (1981). Molybdenum hydroxylases in *Drosophila*. II. Molybdenum cofactor in xanthine dehydrogenase, aldehyde oxidase and pyridoxal oxidase. *Mol. Gen. Genet.* **184**, 92-96.

Warner, C. K., Watts, D. T. and Finnerty, V. (1980). Molybdenum hydroxylases in *Drosophila* I. Preliminary studies of pyridoxal oxidase. *Mol. Gen. Genet.* **180**, 449-453.